

01 Jul 2008

Relation between Channel and Spatial Mesoscopic Correlations in Volume-Disordered Waveguides

Alexey Yamilov

Missouri University of Science and Technology, yamilov@mst.edu

Follow this and additional works at: https://scholarsmine.mst.edu/phys_facwork



Part of the [Physics Commons](#)

Recommended Citation

A. Yamilov, "Relation between Channel and Spatial Mesoscopic Correlations in Volume-Disordered Waveguides," *Physical Review B: Condensed Matter and Materials Physics*, American Physical Society (APS), Jul 2008.

The definitive version is available at <https://doi.org/10.1103/PhysRevB.78.045104>

This Article - Journal is brought to you for free and open access by Scholars' Mine. It has been accepted for inclusion in Physics Faculty Research & Creative Works by an authorized administrator of Scholars' Mine. This work is protected by U. S. Copyright Law. Unauthorized use including reproduction for redistribution requires the permission of the copyright holder. For more information, please contact scholarsmine@mst.edu.

Relation between channel and spatial mesoscopic correlations in volume-disordered waveguides

Alexey Yamilov*

Department of Physics, Missouri University of Science and Technology, Rolla, Missouri 65409, USA

(Received 29 April 2008; published 3 July 2008)

We investigate the relationship between channel and spatial mesoscopic correlations in volume-disordered waveguides. We emphasize the importance of the surface escape function, which describes the distribution of transmitted flux among different channels, and we derive expressions for spatial field and intensity correlation functions directly from the channel ones.

DOI: 10.1103/PhysRevB.78.045104

PACS number(s): 42.25.Dd, 42.25.Bs, 73.23.-b

I. INTRODUCTION

Mesoscopic fluctuations, such as universal conductance fluctuations,¹ are rooted in nonlocal correlations^{2,3} that appear due to the interference effects when a wave undergoes multiple-scattering events in a random medium. Although common to both electrons and electromagnetic (EM) waves, the latter gives more detailed information about transport,^{4,5} for example, the mesoscopic correlation of optical fields leads to readily observable speckles.⁶

The ability to study the localization-delocalization transition as a function of system length, made the quasi-one-dimensional (Q1D) geometry (a disordered wire/waveguide) a fruitful test bed for studying mesoscopic phenomena.⁷⁻⁹ Due to quantization of the transverse momentum, wave transport can be described in terms of a transmission matrix t_{ab} , which is related to the angular transmission coefficient $T_{ab}=|t_{ab}|^2$. The latter measures the flux transmitted in channel b when a unit of flux enters via channel a . Summing over the channel indices gives the transmission $T_a=\sum_b T_{ab}$ and the dimensionless conductance:¹⁰

$$T = \sum_{ab} T_{ab} = \sum_{ab} k_a k_b \mathcal{T}_{ab}; \quad g \equiv \langle T \rangle. \quad (1)$$

Here the k_a are longitudinal components of the momentum, necessary for the proper¹¹ treatment of incoming/outgoing fluxes, and \mathcal{T}_{ab} is the squared amplitude of mode b . For EM waves, T_{ab} , T_a , and T are directly measurable.^{12,13}

Diagrammatic¹ and Dorokhov-Mello-Pereyra-Kumar (DMPK) (Refs. 14 and 15) techniques were highly successful in studying mesoscopic phenomena and were applied to investigate the nonlocal correlations.^{16,17} In the framework of DMPK theory, the correlations in fluxes exiting random medium through different momentum channels were obtained¹⁷ as

$$\langle T_{ab} T_{a'b'} \rangle_{\text{DMPK}} = \frac{\langle T \rangle^2}{N^4} [A^{(c)} \delta_{aa'} \delta_{bb'} + B^{(c)} (\delta_{aa'} + \delta_{bb'}) + A^{(c)}], \quad (2)$$

where N is the number of channels in the waveguide. Although the coefficients $A^{(c)}$ and $B^{(c)}$ depend on the sample length, the structure of Eq. (2) remains the same. For comparison with microwave experiments, the correlation between intensities transmitted from \mathbf{R}_0 and $\mathbf{R}_0 + \Delta \mathbf{R}$ on the input surface and measured at two spatially separated points

\mathbf{r}_0 and $\mathbf{r}_0 + \Delta \mathbf{r}$ at the output surface of random medium can be obtained^{18,19} as

$$\frac{\langle I(\mathbf{R}_0 + \Delta \mathbf{R}, \mathbf{r}_0 + \Delta \mathbf{r}) I(\mathbf{R}_0, \mathbf{r}_0) \rangle}{\langle I(\mathbf{R}_0, \mathbf{r}_0) \rangle^2} = A^{(r)} f^2(\Delta R) f^2(\Delta r) + B^{(r)} \times [f^2(\Delta R) + f^2(\Delta r)] + A^{(r)}, \quad (3)$$

where $f(\Delta r)$ is a field correlation function,²⁰ which takes the form,

$$f(\Delta r) \equiv \frac{\langle E(\mathbf{R}_0, \mathbf{r}_0 + \Delta \mathbf{r}) E^*(\mathbf{R}_0, \mathbf{r}_0) \rangle}{\langle I(\mathbf{R}_0, \mathbf{r}_0) \rangle} = \begin{cases} \frac{\pi \Delta_B J_0(k \Delta r) + 2 \sin(k \Delta r)/k \Delta r}{\pi \Delta_B + 2} & 2D \\ \frac{2J_1(k \Delta r)/k \Delta r + 2 \Delta_B \sin(k \Delta r)/k \Delta r}{1 + 2 \Delta_B} & 3D, \end{cases} \quad (4)$$

at the surface of the random medium.^{21,22} In this expression, $J_n(x)$ are Bessel functions of the first kind, $k=2\pi/\lambda$ is the wave number, and $\Delta_B=z_B/\ell$ is the extrapolation length z_B ^{5,23-25} measured in units of the transport mean free path (MFP) ℓ .

In this work we show that although Eqs. (2) and (3) share structural similarity, one does not follow from the other. The same conclusion holds for the field correlation functions [Eq. (4)] and the DMPK prediction,

$$\langle t_{ab} t_{a'b'} \rangle_{\text{DMPK}} = \frac{\langle T \rangle}{N^2} \delta_{aa'} \delta_{bb'}. \quad (5)$$

We also show that the agreement can be achieved with an *ad hoc* multiplicative correction of the DMPK result [Eqs. (2) and (5)]. The corrections are given by the surface escape function,^{5,25,26} also known as a Chandrasekhar function.²⁷ With such correction, we derive Eqs. (3) and (4) directly from the corrected version of Eqs. (2) and (5).

To begin, we first note the effects of several phenomena that occur in/due to the proximity of sample boundary that have been studied in the context of mesoscopic transport: (i) The very definition of dimensionless conductance²⁸ depends on the treatment of leads (sections of the waveguide without scattering centers) and attached reservoirs;¹⁰ It has been shown¹¹ that Eq. (1) describes the experimentally relevant situations; (ii) Tunneling through an interface barrier and the

concept of “sticking probabilities” is a convenient method of describing coupling to the mesoscopic quantum dot systems,^{9,29} however, it is not directly relevant in context of this work; (iii) Diffusion approximation breaks down at the distances on the order of ℓ from the boundaries of random medium. However, flux-conserving diffusive treatment (an approximation) is possible by requiring the intensity to turn into zero at the distance z_B outside of the sample;^{5,23,25} (iv) Related to (iii), it has been shown^{5,21,25–27} that the energy fluxes are not distributed equally among the transverse momentum channels, and $\langle T_{ab} \rangle = (\langle T \rangle / N^2) \rho_a \rho_b$. Here $\rho_a \neq 1$ is the surface escape function. This is indeed a surface effect because ρ_a is independent of the system length.²⁶ In this paper, we argue that the equivalent channel approximation (ECA) of the DMPK approach is the source of the disagreement between Eqs. (2) and (5) and Eqs. (3) and (4), because it leads to $\rho_a = 1$.

II. NUMERICAL METHOD

In our numerical simulation we consider a two-dimensional (2D) waveguide filled with a random medium disordered array of parallel dielectric cylinders filling the space between two metallic plates. We use a finite difference time-domain method to calculate the response of our system to pulsed excitation, followed by Fourier transformation, which gives us the desired continuous-wave response²² so that t_{ab} can be computed.³⁰ Because the system studied is Q1D, samples with values of g in the range (0.4–4) were obtained by varying the lengths L of the random medium. To ensure that the results obtained do not depend on the microscopic structure of disorder, we operate in the regime of locally weak disorder, $k\ell \gg 1$. To analyze statistics of mesoscopic transport, ensembles of 10^4 – 10^5 random realizations were considered.

III. ON APPLICABILITY OF EQUIVALENT CHANNEL APPROXIMATION

DMPK describes Q1D random medium as a sequence of macroscopically thin slices. It assumes that after scattering in one slice, all transverse momentum channels become completely mixed and, thus, are statistically equivalent. Mathematically, each slice is described by a random transfer matrix with only time-reversal and flux conservation being the constraints.⁷ This isotropy assumption is a mathematically convenient ansatz but it lacks a microscopic foundation.^{26,31} The obtained results depend only on the number of channels, N , and are independent of the dimensionality of the waveguide (and, in three-dimensional (3D), also of its shape).

The validity of the isotropy assumption, or ECA, was questioned before^{26,31,32} and has recently received a renewed focus.³³ It has been linked to DMPKs inability^{31,33} to adequately describe diffusion in the transverse direction, as well as to the difference in the definitions of the mean-free path in DMPK and in transport theory.^{9,26} The modified DMPK formalism, free of the ECA, yields³³ complex equations, which resist an analytical treatment.

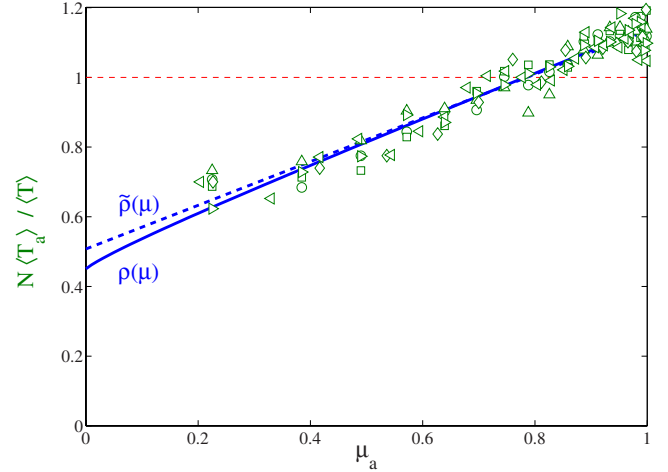


FIG. 1. (Color online) Mean value of transmission normalized by the conductance $\langle T_a \rangle / (\langle T \rangle / N)$ as obtained from numerical simulations in samples with different N , g , and ℓ : (i) \circ — $N=19$ and $g=3.5$; (ii) \square — $N=19$ and $g=1.5$; (iii) \triangle — $N=19$ and $g=0.5$; (iv) \diamond — $N=15$ and $g=0.8$; (v) \triangleleft — $N=28$ and $g=3.0$; and (vi) \triangleright — $N=19$ and $g=4.5$, with ℓ being twice as long as in the previous samples [(i)–(v)]. The data agree with $\rho(\mu)$ given by Eq. (7) and its approximation $\tilde{\rho}(\mu, \Delta_B=0.818)$ (thick solid and dashed lines) *without any adjustable parameters*. Thin dashed line (a constant) depicts the equivalent channel approximation used in DMPK.

A. Channel dependence of $\langle T_{ab} \rangle$

Here, we directly verify earlier reports^{25,26,32,33} that the angular transmission has strong channel dependence. Furthermore, we show, c.f., Fig. 1, that the dependence,

$$\langle T_{ab} \rangle = \frac{\langle T \rangle}{N^2} \rho_a \rho_b, \quad (6)$$

is described by the Chandrasekhar function as found for both the slab⁵ and waveguide²⁶ geometries,

$$\rho(\mu) = C \exp \left[-\frac{\mu}{\pi} \int_0^{\pi/2} \frac{\ln(1 - \cos \beta (\beta / \sin \beta)^{D-2})}{\cos^2 \beta + \mu^2 \sin^2 \beta} d\beta \right], \quad (7)$$

where $D=2,3$ is the dimensionality of the waveguide, $\rho_a \equiv \rho(k_a/k)$, and C is chosen so that ρ_a is normalized $\sum_a \rho_a = N$. Throughout this work, $\langle \dots \rangle$ implies averaging only over disorder configurations for given channel indices $\{a, b\}$. The agreement between Eq. (6) and the numerical data in Fig. 1 is achieved *with no adjustable parameters* for samples with different N , g , and ℓ , with only the condition $L \gg \ell$ to avoid the ballistic regime.²⁶ The deviations from ρ in Fig. 1 are attributed to limited statistics and the finite number N of channels.

Such significant channel dispersion should not come as a surprise as it reflects fundamental wave coherence properties³⁴ and has a long history in radiative transfer theory (RTT).²⁷ For either the slab geometry or the Q1D geometry with $N \gg 1$, $\tilde{\rho}(\mu) \propto \mu + \Delta_B$ is known to be a good approximation with $\Delta_B = z_B / \ell$ as before. Δ_B equals to 0.818 and 0.710 (in 2D and 3D, respectively) arise in RTT, whereas $\Delta_B = \pi/4 \approx 0.785$ and $2/3 \approx 0.667$ are obtained in the diffusion approximation.^{5,25,26} Also, the persistent channel depen-

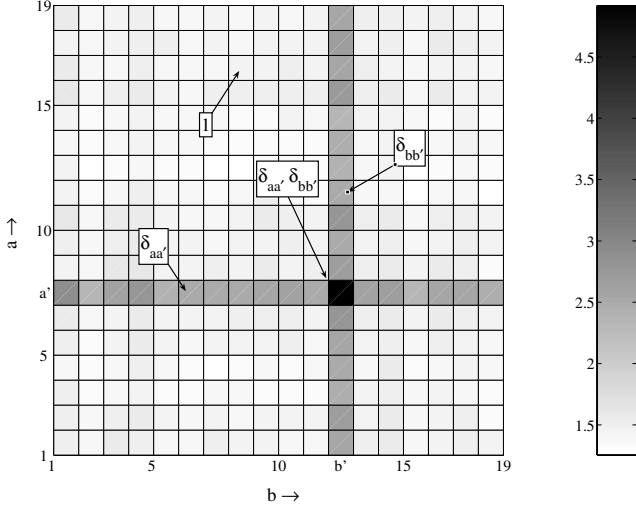


FIG. 2. Channel intensity correlations $\langle T_{ab}T_{a'b'} \rangle$ normalized by $\langle T_{ab} \rangle$ and $\langle T_{a'b'} \rangle$ to remove dependence on $\rho_{a,b}$. General structure of the resulting correlator is described by Eq. (9) and remains the same in all studied samples, regardless of g . A sample with $g=0.4$ and $N=19$ is shown in the figure as an example. To visualize the four-dimensional array $a'=7$, $b'=12$ was selected.

dence of $\langle T_a \rangle$ was observed in the simulations of Ref. 35 but was interpreted as a finite N effect.

B. Channel-channel correlations

Diagrammatic perturbative calculations of the channel correlations in the slab geometry^{4,5,16} give a general relation $\langle T_{ab}T_{a'b'} \rangle \propto \langle T_{ab} \rangle \langle T_{a'b'} \rangle$. Here a, b denote different transverse momenta. The averages $\langle T_{ab} \rangle$ appear when incoming and outgoing paths are paired into diffusons⁵—the only contributions that survive averaging over disorder. Therefore, the nontrivial channel dependence discussed in the above section is expected to affect the channel-channel correlation as well. Our numerical simulation in Fig. 2 show that DMPKs expressions for $\langle T_{ab}T_{a'b'} \rangle_{\text{DMPK}}$ and $\langle t_{ab}t_{a'b'} \rangle_{\text{DMPK}}$, c.f., Eqs. (2) and (5), should be modified to include the multiplicative contribution by the escape function as

$$\langle t_{ab}t_{a'b'}^* \rangle = \frac{\langle T \rangle \rho_a \rho_b}{N^2} \delta_{aa'} \delta_{bb'}, \quad (8)$$

$$\langle T_{ab}T_{a'b'} \rangle = \frac{\langle T \rangle^2 \rho_a \rho_b \rho_{a'} \rho_{b'}}{N^4} [A^{(c)} \delta_{aa'} \delta_{bb'} + B^{(c)} (\delta_{aa'} + \delta_{bb'}) + A^{(c)}]. \quad (9)$$

Upon multiplication by $\rho_{a,b}$ s, the correlations regain a dependence on waveguide dimensionality and shape (in 3D). This is in contrast to DMPK where only the number of channels enters as a sole parameter.

IV. STATISTICS OF TRANSMISSION COEFFICIENTS

The fact that the ensemble-averaged quantity T_{ab} has a dependence on channel indices [Eq. (6)] makes one also question DMPK's assumption of the *statistical* equivalence

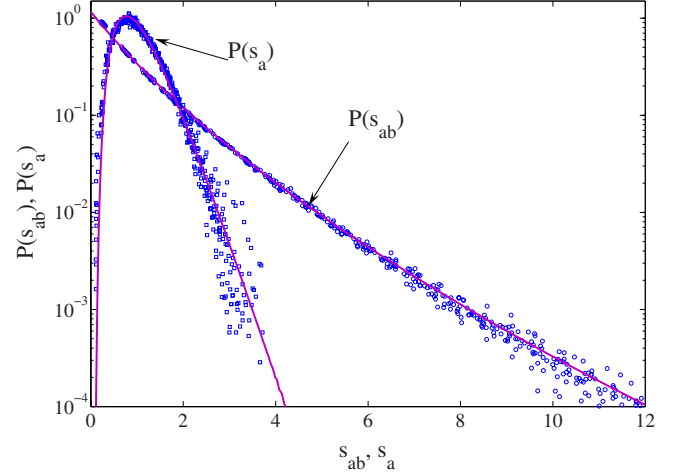


FIG. 3. (Color online) To demonstrate the statistical equivalence of the *normalized* transmission coefficients, two groups of $a=[1..N]$ histograms $P(s_{ab} \equiv T_{ab}/\langle T_{ab} \rangle)$ (with b set to one as an example) and $P(s_a \equiv T_a/\langle T_a \rangle)$ are depicted for the sample with $g=3.5$ and $N=19$. Both groups are successfully fitted by expressions obtained in Ref. 37 with the help of random matrix theory.

of different channels. This is no longer a trivial question because, e.g., in surface disordered waveguides, a strong channel dependence of the MFP can even lead to the coexistence of diffusive and localized regimes³⁶ in different channels of the same sample. However, in the case of volume-disordered waveguide (considered in this work) disorder-induced channel mixing is expected²⁶ to lead to some equilibration for $L \gg \ell$. Although independence of ρ_a in Eq. (6) of g and L may be considered a manifestation of equilibration, it does not require a similarity of *statistics* in different channels.

Our simulations demonstrate, c.f., Fig. 3, that all channels indeed become statistically equivalent when the transmission coefficients are normalized by their ensemble averages. In other words, $P(s_{ab} \equiv T_{ab}/\langle T_{ab} \rangle)$ and $P(s_a \equiv T_a/\langle T_a \rangle)$ are independent of channel indices. It suggests that removing the $\rho_{a,b}$ factor is sufficient to enforce the ECA. It should be noted that although the same notation s_{ab} was also used in an analysis of microwave experiments,¹² its definition is quite different. There, s_{ab} was defined as the ratio between local *intensity* to its ensemble-averaged value. Equivalence of the statistics of the normalized intensity at different spatial points does not imply statistical equivalence of the normalized angular-resolved transmission coefficient $s_{ab} \equiv T_{ab}/\langle T_{ab} \rangle$. The latter follows directly from our numerical simulations (Fig. 3).

The results of Fig. 3 suggest that ECA should be applicable to the renormalized transmission matrix $\sigma_{ab} = t_{ab}/\langle T_{ab} \rangle^{1/2} \propto t_{ab}/[\rho_a \rho_b]^{1/2}$. It is thus tempting to associate σ_{ab} with $t_{ab}^{(\text{DMPK})}$ in the DMPK approach and generate the corresponding angular transmission, the transmission, and the conductance. However, one can see that $s_{ab} \equiv |\sigma_{ab}|^2$ is no longer required to obey the same composition rules $s_a \neq \frac{1}{N} \sum_b s_{ab}$ as the original quantities $T_a = \sum_b T_{ab}$ (the unimportant N^{-1} factor is due to the normalization). Indeed,

$$\frac{1}{N} \sum_b s_{ab} = \frac{N}{\langle T \rangle \rho_a} \sum_b \frac{T_{ab}}{\rho_b} \neq s_a = \frac{N}{\langle T \rangle \rho_a} \sum_b T_{ab}. \quad (10)$$

Note an additional ρ_b^{-1} factor in the expression that involves s_{ab} . We can quantify the mismatch by introducing the quantity,

$$\delta s_a^2 = \left\langle \left(s_a - \frac{1}{N} \sum_b s_{ab} \right)^2 \right\rangle > 0, \quad (11)$$

which is not equal to zero due to presence of mesoscopic correlations in different channels discussed in the previous section. Knowledge of Eq. (9) is needed to derive the following scaling relations:

$$\delta s_a^2 = [A^{(c)} + B^{(c)}] \frac{\alpha - 1}{N}, \quad (12)$$

where $\alpha = (1/N) \sum_a \rho_a^2$. The numerical value of α can be computed in the $N \rightarrow \infty$ limit, when \sum_a can be replaced with an appropriate integration with a continuous function $\rho(\mu)$ given by Eq. (7). We find α to be 1.022 and 1.035 for 2D and 3D waveguides, respectively. Thus, $\alpha - 1 > 0$.

Importantly, the exact cancellation of $O(N^0)$ contributions to Eq. (12) occurred because the channel-channel correlations have the particular form given by Eq. (9). One can easily verify that the same conclusion can be made for quantities $\frac{1}{N} \sum_a s_a$ and $s = 1 / \langle T \rangle \sum_{ab} T_{ab}$. The remaining $O(N^{-1})$ term is nonzero because of inapplicability of the ECA, $\rho_a \neq 1$, which leads to $\alpha - 1 \neq 0$.

Because of cancellation of the $O(N^0)$ terms in Eq. (12), the deviations vanish in the $N \rightarrow \infty$ limit. Therefore, in volume-disordered waveguides with a large number of open channels we expect the quantities:

$$t_{ab}^{(\text{DMPK})}, \quad T_{ab}^{(\text{DMPK})}, \quad T_a^{(\text{DMPK})}, \quad T^{(\text{DMPK})}, \quad (13)$$

to have the same statistical properties as

$$\frac{t_{ab}}{[\rho_a \rho_b]^{1/2}}, \quad \frac{T_{ab}}{\rho_a \rho_b}, \quad \frac{T_a}{\rho_a}, \quad T, \quad (14)$$

respectively. This is the main conclusion of this section.

V. SPATIAL CORRELATIONS

In the previous sections we found the corrected channel correlation functions Eqs. (8) and (9) and verified that with the proper renormalization [Eqs. (13) and (14)] equivalent channel approximation used in the DMPK approach can be applicable. We will now use Eqs. (8) and (9) as the starting point for deriving the spatial field and intensity correlation functions.

The purpose of this exercise is threefold. First, we want to confirm that the obtained correction is consistent with the diagrammatic Green's function results, Eqs. (3) and (4). Second, we would like to establish the relation between $A^{(c)}$, $B^{(c)}$ and $A^{(r)}$, $B^{(r)}$. Finally, using the fact that Eq. (9) was derived nonperturbatively,¹⁷ we would like to show that Eq. (3) is applicable for systems with any value of dimensionless

conductance g . The latter is important because a previous derivation^{18,19} of this equation relied on the smallness of g^{-1} .

A. Field correlations

The electric field at \mathbf{r} on the output surface of the sample produced by a point source placed at \mathbf{R} on the input surface can be related to the complex transmission matrix t_{ab} as

$$E(\mathbf{R}, \mathbf{r}) = \sum_{ab} \frac{\chi_a(\mathbf{R})}{k_a^{1/2}} t_{ab} \frac{\chi_b(\mathbf{r})}{k_b^{1/2}}, \quad (15)$$

where $\chi_a^{(2D)}(\mathbf{r}) = \sqrt{2/W} \sin(\pi/Way)$ is (for a 2D waveguide of width W) the transverse mode of the waveguide and $1 \leq a \leq N$ is an integer used to enumerate the mode. In obtaining the above equation we resolved the delta function into transverse modes on the input surface. $(k_a k_b)^{-1/2}$ appeared because t_{ab} by itself describes the fluxes and not the fields. In the next step we write $E(\mathbf{R}_0 + \Delta \mathbf{R}, \mathbf{r}_0 + \Delta \mathbf{r}) E^*(\mathbf{R}_0, \mathbf{r}_0)$ in terms of transfer-matrix elements and perform two averages. The first is averaging over the statistical ensemble of disorder realizations as in Eq. (8). After this we further average over the cross section of the waveguide. The latter eliminates the dependence on \mathbf{R}_0 and \mathbf{r}_0 . As a result we obtain,

$$\begin{aligned} & \frac{\langle E(\mathbf{R}_0 + \Delta \mathbf{R}, \mathbf{r}_0 + \Delta \mathbf{r}) E^*(\mathbf{R}_0, \mathbf{r}_0) \rangle}{\langle I(\mathbf{R}_0, \mathbf{r}_0) \rangle} \\ &= f(\Delta \mathbf{R}) \times f(\Delta \mathbf{r}) \\ &= \left[\frac{1}{\gamma} \sum_a \frac{\rho_a}{\mu_a} \chi_a(\Delta \mathbf{R}) \right] \left[\frac{1}{\gamma} \sum_b \frac{\rho_b}{\mu_b} \chi_b(\Delta \mathbf{r}) \right], \quad (16) \end{aligned}$$

where the normalization constant γ is given by

$$\gamma = \sum_a \frac{\rho_a}{\mu_a}. \quad (17)$$

For a waveguide with a large number of channels, the summation in Eq. (16) can be transformed to a continuous integral, which depends on the dimensionality of the system (2D and 3D, respectively) as

$$f(\Delta r) \propto \int_0^1 \frac{\rho(\sqrt{1-s^2})}{\sqrt{1-s^2}} \left\{ \cos(ks\Delta r) \right\} \left\{ sJ_0(ks\Delta r) \right\} ds, \quad (18)$$

without the normalization. Substitution of $\tilde{\rho}(\mu) \propto \mu + \Delta_B$ in the integrand and a subsequent integration gives *exactly* Eq. (4). This is the result sought and proves that the corrected Eq. (8) is consistent with Eq. (4).

Finally, we would like to comment on the physical meaning of the ECA in the context of the spatial field correlation function. The integral in Eq. (18) can be reevaluated under the ECA, $\rho_a \equiv 1$. We find,

$$f_{\rho_a \equiv 1}(\Delta r) = \begin{cases} J_0(k\Delta r) & 2D \\ \sin(k\Delta r)/k\Delta r & 3D. \end{cases} \quad (19)$$

The expression obtained coincides with the results found in Ref. 20 for the spatial field correlation function *inside the random medium* if a multiplicative factor $\exp[-\Delta r/2\ell]$ is

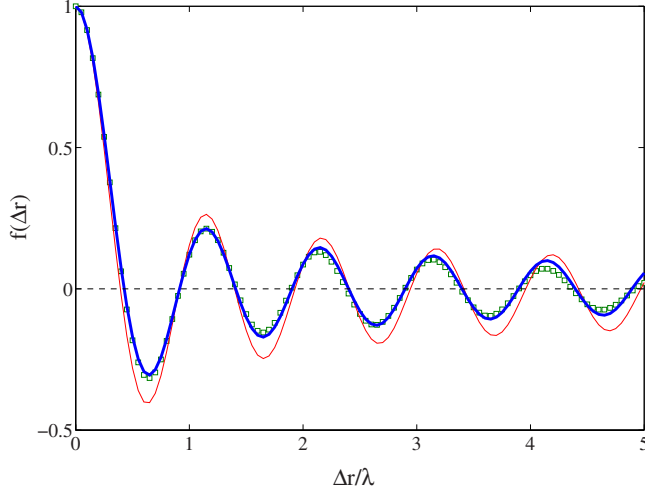


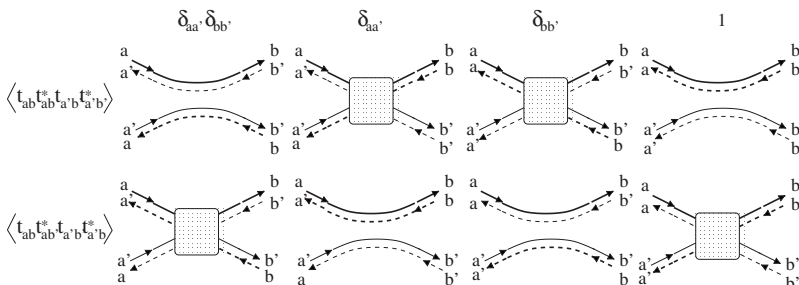
FIG. 4. (Color online) Squares depict the spatial field correlation function (defined in Eq. (4)) obtained in numerical simulation in the sample with $N=19$ and $g=1.5$. The agreement with the right-hand side of Eq. (4) (thick solid line) is reached without any fitting parameters. Δ_B is set to 0.818 as found in RTT. No agreement is found with the thin solid line that depicts the expression in Eq. (19) found in the equivalent channel approximation.

included. For 3D systems, the difference between Eqs. (19) and (4) has been recognized in Ref. 21, where an argument has been presented on why field correlations should not depend on ℓ explicitly, as in Ref. 20.

The expression in Eq. (4) for the spatial field correlation function has been tested in both numerical simulations³⁸ and experiment.³⁹ Figure 4 shows excellent agreement between our numerical data and Eq. (4) with no adjustable parameters. The parameter Δ_B was set to 0.818 as predicted by RTT. In contrast, Eq. (19) could not fit the data in Fig. 4. We attribute this to the inapplicability of the $\rho_a \equiv 1$ approximation (ECA) made in its derivation.

B. Intensity correlations

As in the case of field correlations above, the starting point in obtaining the spatial intensity correlator is Eq. (15). Using the definition, as in Eq. (3), we see that it involves the channel correlator $\langle t_{a_1 b_1}^* t_{a_2 b_2}^* t_{a_3 b_3}^* t_{a_4 b_4}^* \rangle$. For waveguides filled with a weakly scattering random medium ($k\ell \gg 1$), as considered in this work, a nonzero contribution is obtained only when the channel indices are paired into diffusion contributions. We find four possible pairings,



$$\begin{aligned} & \delta_{a_1 a_2} \delta_{b_1 b_2} \delta_{a_3 a_4} \delta_{b_3 b_4} + \delta_{a_1 a_4} \delta_{b_1 b_4} \delta_{a_2 a_3} \delta_{b_2 b_3} \\ & + \delta_{a_1 a_2} \delta_{b_1 b_4} \delta_{a_3 a_4} \delta_{b_2 b_3} + \delta_{a_1 a_4} \delta_{b_1 b_2} \delta_{a_2 a_3} \delta_{b_3 b_4}. \end{aligned} \quad (20)$$

The first two lead to Eq. (9), whereas the last two require knowledge of the new correlator $\langle t_{ab}^* t_{a'b}^* t_{a'b'}^* t_{a'b}^* \rangle$. In the $g \gg 1$ limit, its leading contributions can be analyzed using diagrammatic technique as in Ref. 19. By comparing the diagrams in two types of correlators in Fig. 5, we found the following correspondence:

$$\begin{aligned} \langle t_{ab}^* t_{a'b}^* t_{a'b'}^* t_{a'b}^* \rangle &= \frac{\langle T \rangle^2}{N^4} \rho_a \rho_b \rho_{a'} \rho_{b'} \\ &\times [B^{(c)} \delta_{aa'} \delta_{bb'} + A^{(c)} (\delta_{aa'} + \delta_{bb'}) + B^{(c)}], \end{aligned} \quad (21)$$

with the same coefficients $A^{(c)}$ and $B^{(c)}$ as in Eq. (9). This finding is fully supported by our simulations for all studied samples.

Further calculations include the following steps: First, we evaluate four contributions in Eq. (20) and substitute the appropriate correlators from Eqs. (9) and (21). Then we average over the midpoint positions \mathbf{R}_0 and \mathbf{r}_0 and normalize the expression by $\langle I(\mathbf{R}_0, \mathbf{r}_0) \rangle^2$. We get,

$$\begin{aligned} & \frac{\langle I(\mathbf{R}_0 + \Delta \mathbf{R}, \mathbf{r}_0 + \Delta \mathbf{r}) I(\mathbf{R}_0, \mathbf{r}_0) \rangle}{\langle I(\mathbf{R}_0, \mathbf{r}_0) \rangle^2} \\ &= A^{(c)} f^2(\Delta R) f^2(\Delta r) + B^{(c)} [f^2(\Delta R) + f^2(\Delta r)] + A^{(c)}, \end{aligned} \quad (22)$$

with the same $f(\Delta r)$ as in Eq. (16). Also, we retained only the terms of $O(1/N^0)$. Comparing Eqs. (3) and (22), we obtain the desired result $A^{(r)} \equiv A^{(c)}$ and $B^{(r)} \equiv B^{(c)}$.

VI. CONCLUSION

In this work we studied both analytically and numerically field and intensity correlations in wave transport through volume-disordered waveguides. It was shown that channel correlation functions obtained in the framework of the DMPK formalism, Eqs. (2) and (5), are not consistent with their spatial counterparts found with the Green's function technique [Eqs. (3) and (4)]. We related the discrepancy to the inapplicability of the equivalent channel approximation in the DMPK. We demonstrated that an agreement can be recovered with the help of a surface escape function [Eqs. (6) and (7)], which describes the distribution of transmitted flux among different channels of the waveguide. As a result, we

FIG. 5. Two types of channel correlators and their leading diagrams in a $1/g$ perturbation series that appear in the derivation of the spatial intensity correlation function [Eq. (22)]. The known expression for $\langle T_{ab} T_{a'b'} \rangle$ is shown in the first line, see e.g. (Ref. 5). Leading contributions to the correlator $\langle t_{ab}^* t_{a'b}^* t_{a'b'}^* t_{a'b}^* \rangle$ can be obtained by swapping the incoming and outgoing indices as shown in the second row, Eq. (21) follows.

derived expressions for spatial field and intensity correlation functions from the corrected channel functions [Eqs. (9) and (8)]. In the derivation we encountered new correlator [Eq. (21)], which was found with the diagrammatic analysis [Fig. 5]. The results obtained were verified in numerical simulations.

We also related the coefficients that enter into the expression for the channel [Eq. (8)] and spatial intensity [Eq. (3)] correlations, namely, $A^{(r)} \equiv A^{(c)}$ and $B^{(r)} \equiv B^{(c)}$. Importantly, because the expression for the channel intensity correlations is known nonperturbatively,¹⁷ our derivation shows that Eq. (3) should hold also in the localized regime. Its applicability

in the crossover and the localized regime was indeed found in numerical simulations²² and microwave experiments.⁴⁰

Albeit the studied correlations are directly measurable only for electromagnetic waves. Our results are also applicable to noninteracting electronic systems, e.g., a volume-disordered wire, where time-reversal symmetry is preserved and dephasing mechanisms can be neglected.

ACKNOWLEDGMENT

The author acknowledges the support of the National Science Foundation Grant No. DMR-0704981.

*yamilov@mst.edu

- ¹ *Mesoscopic Phenomena in Solids*, edited by B. L. Altshuler, P. A. Lee, and R. A. Webb (North Holland, Amsterdam, 1991).
- ² M. J. Stephen and G. Cwilich, *Phys. Rev. Lett.* **59**, 285 (1987).
- ³ R. Pnini and B. Shapiro, *Phys. Rev. B* **39**, 6986 (1989).
- ⁴ R. Berkovits and S. Feng, *Phys. Rep.* **238**, 135 (1994).
- ⁵ M. C. W. van Rossum and Th. M. Nieuwenhuizen, *Rev. Mod. Phys.* **71**, 313 (1999).
- ⁶ *Waves and Imaging Through Complex Media*, edited by P. Sebbah (Kluwer, Dordrecht, 2001).
- ⁷ P. A. Mello and N. Kumar, *Quantum Transport in Mesoscopic Systems* (Oxford University Press, Oxford, 2004).
- ⁸ A. D. Mirlin, *Phys. Rep.* **326**, 259 (2000).
- ⁹ C. W. J. Beenakker, *Rev. Mod. Phys.* **69**, 731 (1997).
- ¹⁰ D. S. Fisher and P. A. Lee, *Phys. Rev. B* **23**, 6851 (1981).
- ¹¹ A. D. Stone and A. Szafer, *IBM J. Res. Dev.* **32**, 384 (1988).
- ¹² M. Stoytchev and A. Z. Genack, *Phys. Rev. Lett.* **79**, 309 (1997); M. Stoytchev and A. Z. Genack, *Opt. Lett.* **24**, 262 (1999).
- ¹³ A. A. Chabanov, M. Stoytchev, and A. Z. Genack, *Nature (London)* **404**, 850 (2000).
- ¹⁴ O. N. Dorokhov, *JETP Lett.* **36**, 318 (1982).
- ¹⁵ P. A. Mello, P. Pereyra, and N. Kumar, *Ann. Phys. (N.Y.)* **181**, 290 (1988).
- ¹⁶ S. Feng, C. Kane, P. A. Lee, and A. D. Stone, *Phys. Rev. Lett.* **61**, 834 (1988).
- ¹⁷ P. A. Mello, E. Akkermans, and B. Shapiro, *Phys. Rev. Lett.* **61**, 459 (1988).
- ¹⁸ P. Sebbah, B. Hu, A. Z. Genack, R. Pnini, and B. Shapiro, *Phys. Rev. Lett.* **88**, 123901 (2002).
- ¹⁹ R. Pnini, in *Waves and Imaging Through Complex Media*, edited by P. Sebbah (Kluwer, Dordrecht, 2001), pp. 391–412.
- ²⁰ B. Shapiro, *Phys. Rev. Lett.* **57**, 2168 (1986).
- ²¹ I. Freund and D. Eliyahu, *Phys. Rev. A* **45**, 6133 (1992).
- ²² S. H. Chang, A. Taflove, A. Yamilov, A. Burin, and H. Cao, *Opt. Lett.* **29**, 917 (2004).
- ²³ A. Ishimaru, *Wave Propagation and Scattering in Random Media* (Academic, New York, 1978).
- ²⁴ A. Lagendijk, R. Vreeker, and P. de Vries, *Phys. Lett. A* **136**, 81 (1989).
- ²⁵ M. B. Hastings, A. D. Stone, and H. U. Baranger, *Phys. Rev. B* **50**, 8230 (1994).
- ²⁶ A. V. Tartakovski, *Phys. Rev. B* **52**, 2704 (1995).
- ²⁷ S. Chandrasekhar, *Radiative Transfer* (Dover, New York, 1960).
- ²⁸ R. Landauer, *Philos. Mag.* **21**, 863 (1970).
- ²⁹ S. Iida, H. A. Weidenmuller, and J. A. Zuk, *Phys. Rev. Lett.* **64**, 583 (1990).
- ³⁰ A. Yamilov and H. Cao, *Phys. Rev. E* **74**, 056609 (2006).
- ³¹ P. A. Mello and S. Tomsovic, *Phys. Rev. Lett.* **67**, 342 (1991).
- ³² P. Garcia-Mochales, P. A. Serena, N. Garcia, and J. L. Costa-Kramer, *Phys. Rev. B* **53**, 10268 (1996).
- ³³ L. S. Froufe-Perez, M. Yezpez, P. A. Mello, and J. J. Saenz, *Phys. Rev. E* **75**, 031113 (2007).
- ³⁴ W. H. Carter and E. Wolf, *J. Opt. Soc. Am.* **65**, 1067 (1975).
- ³⁵ P. Markos and C. M. Soukoulis, *Phys. Rev. B* **71**, 054201 (2005).
- ³⁶ J. A. Sanchez-Gil, V. Freilikher, I. Yurkevich, and A. A. Maradudin, *Phys. Rev. Lett.* **80**, 948 (1998).
- ³⁷ E. Kogan and M. Kaveh, *Phys. Rev. B* **52**, R3813 (1995).
- ³⁸ A. Yamilov, S. H. Chang, A. Burin, A. Taflove, and H. Cao, *Phys. Rev. B* **71**, 092201 (2005).
- ³⁹ P. Sebbah, R. Pnini, and A. Z. Genack, *Phys. Rev. E* **62**, 7348 (2000).
- ⁴⁰ A. A. Chabanov, B. Hu, and A. Z. Genack, *Phys. Rev. Lett.* **93**, 123901 (2004).